Nup120p: A Yeast Nucleoporin Required for NPC Distribution and mRNA Transport

John D. Aitchison, Günter Blobel, and Michael P. Rout

The Laboratory of Cell Biology, Howard Hughes Medical Institute, The Rockefeller University, New York 10021-6399

Abstract. To extend our understanding of the mechanism by which the nuclear pore complex (NPC) mediates macromolecular transport across the nuclear envelope we have focused on defining the composition and molecular organization of the yeast NPC. Peptide sequence analysis of a polypeptide with a M_r of ~100,000 present in a highly enriched yeast NPC fraction identified a novel yeast nucleoporin we term Nup120p. Nup120p corresponds to the open reading frame (ORF) YKL057c identified by the yeast genome sequencing project. The ORF predicts a protein with a calculated molecular mass of 120.5 kD containing two leucine zipper motifs, a short coiled–coil region and limited primary sequence similarity to Nup133p. Nup120p was localized to the NPC using a protein A–tagged chimera in situ by indirect immunofluorescence microscopy. Deletion of the *NUP120* gene caused clustering of NPCs at one side of the nuclear envelope, moderate nucleolar fragmentation and slower cell growth. Transfer of *nup120Δ* cells to 37°C resulted in the nuclear accumulation of poly(A)$^+$ mRNA, extensive fragmentation of the nucleolus, spindle defects, and cell death.

NUCLEAR pore complexes (NPCs)[1] span circular openings in the nuclear envelope (NE) where they govern bidirectional macromolecular traffic between the nucleus and cytoplasm. The NPC is a huge (~125 MD in vertebrates and ~65 MD in yeast) octagonally symmetric cylindrical structure. Investigation of the NPC structure by electron microscopy and high resolution image reconstruction has revealed a complex subunit organization. Four coaxial rings lie parallel to the nuclear envelope and are joined by eight spokes: two morphologically symmetric cytoplasmic and nuclear rings flank the core structure of the NPC at the nuclear and cytoplasmic faces; an outer spoke ring lies within the lumen of the nuclear envelope and a nuclear ring surrounds a central transporter. Eight cytoplasmic filaments and particles emanate from the cytoplasmic ring, and eight filaments attached to the nucleoplasmic ring extend to a distal basket ring and comprise the nuclear basket (Unwin and Milligan, 1982; Jarnik and Aebi, 1991; Goldberg et al., 1992; Hinshaw et al., 1992; Akey and Radermacher, 1993; Ris and Malecki, 1993). The NPC has been estimated to contain at least 40 nucleoporins (nups) and pore membrane proteins (poms) some of which have been identified and molecularly characterized.

Address all correspondence to G. Blobel, The Laboratory of Cell Biology, Howard Hughes Medical Institute, The Rockefeller University, Box 168, 1230 York Ave., New York, NY 10021-6399. Ph.: (212) 327-8097. Fax: (212) 327-7880.

1. *Abbreviations used in this paper*: NE, nuclear envelope; NPC, nuclear pore complex; nup, nucleoporins; ORF, open reading frame; pom, pore membrane proteins; PVDF, polyvinyldiene difluoride membrane; SM, synthetic minimal medium.

Isolation of subcellular fractions enriched in NPCs from vertebrates and yeast as well as genetic analyses of yeast nucleoporins have contributed to the recent rapid identification and characterization of several nucleoporins and pore membrane proteins (reviewed in Rout and Wente, 1994). In addition to the pore membrane proteins, Pom152p (Wozniak et al., 1994), Pom121p (Hallberg et al., 1993), and gp210 (Gerace et al., 1982; Wozniak et al., 1989), nucleoporins are broadly classified into two groups of proteins: those containing repetitive peptide motifs which, in yeast, include Nup1p, Nup2p, Nsp1p, Nup42p, Nup49p, Nup57p, Nup100p, Nup116p, Nup145p, and Nup159p (reviewed in Rout and Wente, 1994; see also Fabre and Hurt, 1994; Gorsch et al., 1995; Grandi et al., 1995; Kraemer et al., 1995; Stutz et al., 1995), and in mammalian cells include p62, Nup98p, Nup153p, Nup214p, and Nup358p (reviewed in Rout and Wente, 1994; see also Fabre and Hurt, 1994; Radu et al., 1995; Wu et al., 1995). Some of these repeat containing proteins have been shown to bind the transport factor karyopherin β and as such may be directly involved in macromolecular transport through the NPC (Radu et al., 1995; Kraemer et al., 1995). The second class of nucleoporins do not contain such repetitive elements and some may play a role in maintaining the complex structure of the NPC. These proteins include Nic96p (Grandi et al., 1993) Nup133p (Doye et al., 1994; Pemberton et al., 1995; Li et al., 1995), Nup82p (Hurwitz and Blobel, 1995), Nup157p, and Nup170p (Aitchison et al., 1995) in yeast and the vertebrate proteins Nup155p (Radu et al., 1993), Nup107p (Radu et al., 1994), and Tpr (Nup266p; Byrd et al., 1995).

© The Rockefeller University Press, 0021-9525/95/12/1659/17 $2.00

In an effort to examine the precise roles of nucleoporins in the subunit organization of the NPC and macromolecular transport processes we have extended our characterization of yeast nucleoporins to a novel essential nucleoporin, termed Nup120p. Nup120p was isolated from a highly enriched yeast NPC fraction and identified by direct microsequencing. The protein shows limited primary sequence similarity to Nup133p (Doye et al., 1994; Pemberton et al., 1995; Li et al., 1995) and contains two leucine zippers and a third potential putative coiled–coil domain. Deletion of the *NUP120* gene causes pores to cluster at one side of the nuclear envelope and, at elevated growth temperatures, poly(A)$^+$ mRNA accumulation in the nucleus, extensive nucleolar fragmentation, spindle defects, and cell death.

Materials and Methods

Yeast Strains and Media

All yeast strains constructed in this study were derived from the strain DF5 (*Mata/Matα ura3-52/ura3-52 his3-Δ200/his3-Δ200 trp1-1/trp1-1 leu2-3,112/leu2-3,112 lys2-801/lys2-801*; Aitchison et al., 1995). NP120-25-3 (*Mata ura3-52 his3-Δ200 trp1-1 leu2-3,112 lys2-80 nup120::URA3*) is a haploid segregant of the heterozygous diploid NP120Δ-25 generated by integrative transformation of the *URA3* gene into the *NUP120* locus of DF5 cells (see below). NP120-A (*Mata/Matα ura3-52/ura3-52 his3-Δ200/his3-Δ200 trp1-1/trp1-1 leu2-3,112/leu2-3,112 lys2-801/lys2-801 nup120-protA (URA3-HIS3)/+*) was created by integrative transformation of the *Staphylococcal* protein A IgG binding domains and the *HIS3* and *URA3* genes at the 3′ end of the *NUP120* open reading frame (ORF) (see below). All strains were grown as described (Sherman et al., 1986) in YPD (1% yeast extract, 2% bactopeptone, and 2% glucose) or synthetic minimal media (SM) supplemented with the appropriate amino acids and 2% glucose at 30°C unless otherwise stated. Procedures for yeast manipulation were conducted as described by Sherman et al. (1986). Yeast were transformed by electroporation (Delorme et al., 1989).

Identification of Nup120p

Proteins comprising a highly enriched yeast nuclear pore complex fraction (~10 mg of total protein) were separated by ion exchange chromatography, reverse phase HPLC, and SDS-PAGE as described (Rout and Blobel, 1993; Wozniak et al., 1994). A protein of this fraction with a M_r of ~100,000 was selected for microsequencing based on its abundance, separation from other proteins of the fraction and cofractionation during the enrichment procedure. Column fractions 46-51 (Rout and Blobel, 1993; cf. Fig. 1 *A*) containing this protein were pooled, separated by SDS-PAGE and transferred electrophoretically to polyvinyldiene difluoride membrane (PVDF). The 100-kD protein was visualized on the membrane with 0.1% amido black in 10% acetic acid, excised, cleaved with endopeptidase Lys-C (Fernandez et al., 1994), and the peptides subjected to NH_2-terminal sequence analysis.

Gene disruption and Protein A Tagging of NUP120

The *NUP120* gene was replaced in the DF5 cells by direct integration of the *URA3* gene using the procedure of Rothstein (1991). The *URA3* gene with flanking *NUP120* DNA sequence was generated by the PCR using the following primers and the plasmid pURAGal (Aitchison et al., 1995) as a template:

sense primer:
5′-CATAAGCATTTTTCAAGAGGTCGCAATTTCACTCG-TACACAACTGACCTATTATGGCATGCCACCGCGGTGG-CGGCCG-3′
antisense primer:
5′-AGTAACCACTTTACTTCCGTTTAGAATCCATTGATCG-TATGCACTATCAAAGCTAGATAACATTTACTTATAATA-CAG-3′

The 5′ regions of the sense and antisense primers correspond to nucleotides −52 to +2 and +3078 to +3019 of *NUP120* (where +1 = A of the initiation codon) while the 3′ end of each primer was designed to prime the synthesis of the *URA3* gene (Rose et al., 1984). The 1.2-kb PCR product was precipitated and transformed directly into DF5 cells and Ura$^+$ transformants were selected on SM-uracil plates. Ura$^+$ strains were analyzed by the PCR using primers within the *URA3* gene (URA700: 5′-GCA-AGGGCTCCCTATCTACTG-3′) (Rose et al., 1984) and 3′ to the *NUP120* ORF (120+: 5′-AGCTCTAGGAACAGTGTCATG-3′). Clones giving the expected 683-bp fragment were sporulated and tetrads were dissected on YPD. All spores were viable in several tetrads; however there was a slow growth phenotype which segregated 2:2 with the *URA3* marker.

A genomic copy of the *NUP120* gene was tagged by a COOH-terminal, in-frame integration of a PCR-derived DNA fragment encoding the IgG binding domains of protein A as previously described (Aitchison et al., 1995). The following primers and the plasmid pProtA/HU were designed to generate a COOH-terminal fusion which places the region encoding the five IgG binding domains of protein A at the 3′ end of *NUP120* followed by the *HIS3* and *URA3* genes:

sense primer:
5′-TACGATCAATGGATTCTAAACGGAAGTAAAGTGGTTACT-TTAACTGATTTAAGAGATGAGTTACGAGGTCTAGGTGAA-GCTCAAAAACTTAAT-3′
antisense primer:
5′-TAATTTAGATTTAAAGTTCAATCTTTTTACTTAAAAAAC-AAACGAAGATCATGGTGCTAATATTCGGATTTTACTTATA-ATACAGTTTTTTAG-3′

The 5′ region of the sense primer corresponds to nucleotides 3040–3111 of the *NUP120* ORF (immediately upstream of the termination codon at nucleotide +3112). The 21 nucleotides at the 3′ region of the sense oligonucleotide correspond to the sequence of protein A beginning at the glycine at amino acid 24 (Uhlen et al., 1984). The 5′ region of the antisense primer corresponds to nucleotides +3236 to +3167 in the 3′ untranslated region of *NUP120*. The PCR product was transformed into DF5 cells as for the disruption. His$^+$, Ura$^+$ colonies were replica plated onto nitrocellulose, grown overnight on nitrocellulose, and probed directly for protein A expression as described (Aitchison et al., 1995).

Immunofluorescence and Electron Microscopy

Immunofluorescence microscopy to detect the Nup120p-protein A chimera was done essentially as previously described (Kilmartin and Adams, 1984; Wente et al., 1992) and visualized using rabbit anti–mouse IgG (preadsorbed against formaldehyde fixed wild-type yeast cells) followed by Cy3 conjugated donkey anti–rabbit IgG antibody (Jackson ImmunoResearch Laboratories, West Grove, PA).

To examine cells for poly(A)$^+$ RNA accumulation and nuclear morphology, NP120-25-3 and DF5 cells were grown in YPD to mid-logarithmic phase at 23°C and transferred to 37°C for the indicated length of time. Cells were fixed for 20–60 min in 4% formaldehyde at room temperature, and processed for either immunofluorescence using an anti-Nop1p mouse monoclonal antibody (D77; Aris and Blobel, 1988), an anti-tubulin rabbit polyclonal antibody (R243; Rout and Kilmartin, 1990), an anti-Nsp1p rabbit polyclonal antibody (EC10-2; Hurt, 1988; Nehrbass, 1990), or an anti-Srp1p rabbit polyclonal antibody (Kap60p; Enenkel et al., 1995) followed, as appropriate, by a Cy3-conjugated donkey anti–mouse IgG antibody, and/or a fluorescein-conjugated donkey anti–rabbit IgG antibody (Jackson ImmunoResearch Laboratories, West Grove, PA), or for in situ hybridization with digoxigenin-labeled oligo(dT)$_{30}$ as previously described (Forrester et al., 1992; Wente and Blobel, 1993). Digoxigenin-labeled (dT)$_{30}$ (20 ng/ml) was visualized after overnight hybridization at 37°C using FITC-labeled anti-digoxigenin antibody (Boehringer Mannheim Corp., Indianapolis, IN).

For electron microscopy, cells were grown in YPD at 23°C, transferred to 37°C for the indicated length of time, and processed for electron microscopy as previously described (Byers and Goetsch, 1991; Wente et al., 1992).

Examination of Synthetic Lethality

Double null mutants of *nup120* and *nup170*, *nup188*, *nup133*, or *pom152* were produced by crossing NP120-25-3 cells with each of the following: PM152-75 (*Matα ade2 ade3 ura3 his3 trp1 leu2 can1 pom152-2::HIS3*), NP170-11.1 (*Matα ade2-1 ura3-1 his3-11,15 trp1-1 leu2-3,112 can1-100*

nup170-1::HIS3), NP188-2.4 (*Matα ade2-1 ura3-1 his3-11,15 trp1-1 leu2-3,112 can1-100 nup188-1::HIS3*) (Aitchison et al., 1995), and *nup133Δ* cells (3–4; *Matα ura3-52 his3-Δ200 trp1-1 leu2-3,112 lys2-80 nup133::HIS3*) (Pemberton et al., 1995). Diploids were selected by complementation of *HIS3* and *URA3* markers. Approximately 20 tetrads from each cross were dissected. Segregants were scored for growth on YPD at 23°C and for both the *HIS3* and *URA3* markers.

Results

Identification of Nup120p

The isolation of a fraction of yeast highly enriched intact NPCs (Rout and Blobel, 1993) has facilitated the identification of a growing number of nucleoporins. We have extended this biochemical approach to the identification and characterization of a novel yeast nucleoporin, termed Nup120p. Separation of the proteins of the highly enriched NPC fraction by anion exchange chromatography followed by HPLC and SDS-PAGE allowed us to identify a polypeptide with an estimated M_r of ~100,000 which co-enriched with NPCs during the isolation (Fig. 1 *A*). Two peptide sequences derived from this polypeptide matched exactly with the ORF YKL057c on the left arm of chromosome XI sequenced in the yeast genome sequencing project (Fig. 1 *B*). Based on its co-isolation with NPCs and in situ evidence described below, we have renamed this ORF, *NUP120.* A search of the GenBank/EMBL/DDBJ and Swiss-Prot databases using the FASTA program failed to identify any extended regions of sequence similarities with other proteins in the database. Interestingly, however, a short region (amino acids 98–420) of Nup133p (Doye et al., 1994; Li et al., 1995) was identified which showed 20% identity and 62% similarity to amino acids 434–763 of Nup120p (Fig. 1 *C*). This region of homology corresponds to the amino-terminal portion of Nup133p which has been previously shown to be required in Nup133p for the spatial distribution of NPCs (Doye et al., 1994). The protein contains no regions of significant hydrophobicity (lacking charged residues) which could act as transmembrane segments (Kyte and Doolittle, 1982) and overall is relatively acidic with a pI of 5.0. In addition, analysis of the protein sequence (Fig. 1 *B*) revealed two potential leucine zipper domains between residues 128–155 and 287–314 (MacPattern; Fuchs, 1991; Alber et al., 1992) and a third heptad repeat with the potential to form a short coiled–coil between amino acids 435 and 465 (MacStripe v1.3.1; Lupas et al., 1991; Knight, 1994). Given their involvement in protein–protein interactions, these domains may interact with other proteins of the NPC thus contributing to its architectural complexity.

Localization of Nup120p to the Nuclear Pore Complex

To determine the subcellular localization of Nup120p, the protein was tagged by a carboxy-terminal fusion with the IgG-binding domains of protein A. The Nup120p-protein A fusion was created by integration of the coding region of protein A immediately 5′ to the stop codon of the genomic copy of *NUP120* thus allowing expression of the chimera under control of its own promoter. Oligonucleotide primers were designed to amplify the protein A gene (and flanking *HIS3* and *URA3* markers) by the PCR. The primers contained approximately 60 nucleotides at their 5′ ends corresponding to the desired site of insertion (Fig. 2 *A*). The PCR product was transformed into DF5 cells and His^+, Ura^+ transformants were selected. Clones bearing the desired fusion product were identified by western blotting and the PCR. Analysis of one of the resulting strains, NP120-A, by indirect immunofluorescence microscopy indicated that the Nup120p–protein A chimera was localized to the nuclear periphery in a punctate staining pattern characteristic of nucleoporins (Fig. 2 *B*). Furthermore, sporulation and tetrad dissection of NP120-A cells indicate that the fusion protein is functional. None of the growth defects or morphological phenotypes associated with the *nup120Δ* strains described below were exhibited by the resulting haploid spores. Immunofluorescent staining of haploid cells containing *NUP120*–protein A replacing the wild type copy of *NUP120* revealed typical NPC staining with the monoclonal antibody mAb192 (Rout and Blobel, 1993; Wente et al., 1993) and subcellular fractionation of these cells showed coenrichment of Nup120p–protein A with the nuclear envelope (data not shown).

Deletion of NUP120 causes Temperature Sensitivity

The gene encoding Nup120p was disrupted in the diploid yeast strain DF5 by integrative transformation of the *URA3* gene (Fig. 3 *A*; see Materials and Methods). The heterozygous diploid *nup120::URA3*/+ strain was sporulated and tetrads were dissected. Four viable spores were recovered from most tetrads; however, the segregants carrying the disruption (*nup120::URA3*) grew much slower and were noticeably larger than the cells with the wild-type *NUP120* gene, and failed to grow when plated at 37°C (Fig. 3 *B*).

To examine this growth defect further, the growth rates and survival of *nup120Δ* (NP120-25-3) cells were monitored over a 24 h period (Fig. 3 *C*). At 23°C *nup120Δ* cells grew with a generation time of approximately 4–5 h compared to approximately 2 h for wild-type cells. After transfer to 37°C the number of *nup120Δ* cells doubled over the first 10–15 h. At both temperatures *nup120Δ* cells appeared larger by light microscopy. The viability of the cells was monitored by removing aliquots from the liquid cultures and plating at 23°C (Fig. 3 *D*). *nup120Δ* cells rapidly lost viability after approximately 10 h at 37°C, and after 24 h, less than 1% of the cells were able to form colonies. The loss of viability of *nup120Δ* cells at 37°C coincides with the strain's generation time, suggesting that cells can undergo only 1–2 divisions before they die at the restrictive temperature.

nup120Δ (*nup120::URA3*) cells were crossed with strains harboring deletions of the genes encoding other NPC proteins in order to examine possible genetic interactions. Crosses were made with *pom152Δ* (PM152-75; *pom152::HIS3*), *nup170Δ* (NP170-11.1; *nup170::HIS3*) (Aitchison et al., 1995), *nup188Δ* (NP188-2.4; *nup188::HIS3*; (Nehrbass, U. S. Maguire, M. P. Rout, G. Blobel, and R. W. Wozniak, manuscript submitted) and *nup133Δ* (3-4; *nup133::HIS3*; Pemberton et al., 1995). Approximately twenty tetrads of each cross were dissected and examined for segregation of markers and viability. In no case could viable haploid strains carrying both markers (His^+, Ura^+) be recovered and each

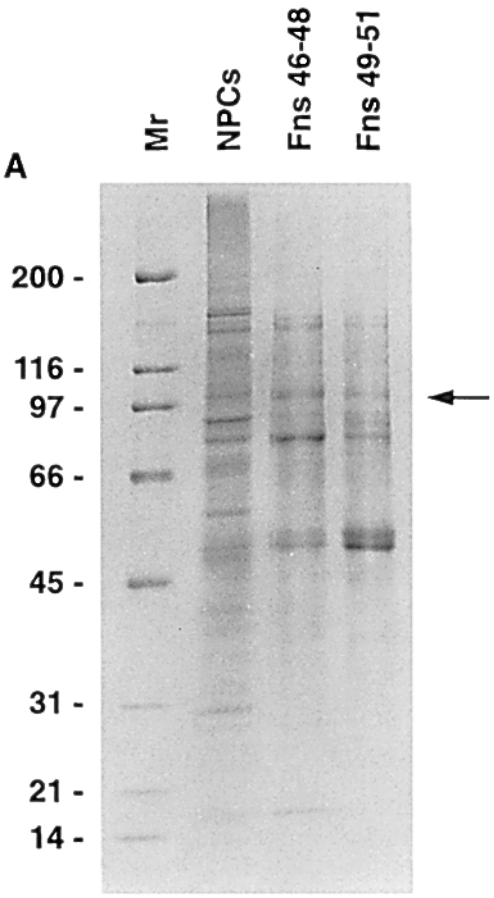

B

```
1     MACLSRIDANLLQYYEKPEPNNTVDLYVSNNSNNNGLKEGDKSISTPVPQPYGSEYSNCL
61    LLSNSEYICYHFSSRSTLLTFYPLSDAYHGKTINIHLPNASMNQRYTLTIQEVEQQLLVN
121   VILKDGSFLTLQLPLSFLFSSANTLNGEWFHLQNPYDFTVRVPHFLFYVSPQFSVVFLED
181   GGLLGLKKVDGVHYEPLLFNDNSYLKKSLTRFFSRSSKSDYDSVISCKLFHERYLIVLTQN
241   CHLKIWDLTSFTLIQDYDMVSQSDSDPSHFRKVEAVGEYLSLYNNTLVTLLPLENGLFQM
301   GTLLVDSSGILTYTFQNNIPTNLSASAIWSIVDLVLTRPLELNVEASYLNLIVLWKSGTA
361   SKLQILNVNDESFKNYEWIESVNKSLVDLQSEHDLDIVTKTGDVERGFCNLKSRYGTQIF
421   ERAQQILSENKIIMAHNEDEEYLANLETILRDVKTAFNEASSITLYGDEIILVNCFQPYN
481   HSLYKLNTTVENWFYNMHSETDGSELFKYLRTLNGFASTLSNDVLRSISKKFLDIITGEL
541   PDSMTTVEKFTDIFKNCLENQFEITNLKILFDELNSFDIPVVLNDLINNQMKPGIFWKKD
601   FISAIKFDGFTSIISLESLHQLLSIHYRITLQVLLTFVLFDLDTEIFGQHISTLLDLHYK
661   QFLLLNLYRQDKCLLAEVLLKDSSEFSFGVKFFNYGQLIAYIDSLNSNVYNASITENSFF
721   MTFFRSYIIENTSHKNIRFFLENVECPFYLRHNEVQEFMFAMTLFSCGNFDQSYEIFQLH
781   DYPEAINDKLPTFLEDLKSENYHGDSIWKDLLCTFTVPYRHSAFYYQLSLLFDRNNSQEF
841   ALKCISKSAEYSLKEIQIEELQDFKEKQHIHYLNLLIHFRMFEEVLDVLRLGHECLSDTV
901   RTNFLQLLLQEDIYSRDFFSTLLRLCNAHSDNGELYLRTVDIKIVDSILSQNLRSGDWEC
961   FKKLYCFRMLNKSERAAAEVLYQYILMQADLDVIRKRKCYLMVINVLSSFDSAYDQWILN
1021  GSKVVTLTDLRDELRGL
```

C

```
Nup120p  434  MAHNEDEEYLANLETILRDVKTAFNEASSI
Nup133p   98  LVNDHKKVYIWNIHSTQKD--TPYITVPFR

Nup120p  464  TLYGDEIILV-NCFQPYNHSLYKLNTTVEN
Nup133p  126  SDDNDEIAVAPRCILTFPATMDESPLALNP

Nup120p  493  WFYNMHSETDGSELFKYLRTLNGFASTLSN
Nup133p  156  ---NDQDETGGLIIIKGSKAIYYEDINSIN

Nup120p  523  DVLRSISKKFLDIITGELPDSMTTVEKFTD
Nup133p  183  NLNFKLSEKFSHEL--ELPINSSGGEK-CD

Nup120p  553  IFKNCLENQFEI-TNL-KILFDEL-NSFDI
Nup133p  210  LMLNCEPAGIVLSTNMGRIFFITIRNSMGK

Nup120p  580  PVV-LNDLINNQMKPGIFWKKDFISAIKFD
Nup133p  240  PQLKLGKLLNKPFKLGI-WSKIFNTN----

Nup120p  609  GFTSIISLESLHQLLSIHYRITLQVLLTFV
Nup133p  265  --SSVVSLRN-GPILGKGTRLVYITTNKGI

Nup120p  639  LFDLDTEIFGQHISTLLDLHYKQFLLLNLY
Nup133p  292  FQTWQLSATNSHPTKLIDVNIYEAILESL-

Nup120p  669  RQDKCLLAEVLLK--------DSSEFSFG
Nup133p  321  -QDLYPFAHGTLKIWDSHPLQDESSQLFLS

Nup120p  690  VKFFNYGQLIAYIDSLNSNVYNASITENSF
Nup133p  350  SIYDSSCNETYYI--LSTIIFDSS--SNSF

Nup120p  720  FMTFFRSYIIENTSHKNIR--FFLENVECP
Nup133p  376  TIFSTYRL-NTFMESITDTKFKPKIFIPQM

Nup120p  748  FYLRHNEVQEFMFAMT
Nup133p  405  ENANDTNEVTSILVMF
```

Figure 1. Identification of Nup120p. Fractions 46–48 and 49–51 of HPLC-separated highly enriched NPCs (Rout and Blobel, 1993) were analysed by SDS-PAGE revealing an intense Coomassie-stained band at M_r ~100,000 (*A*, *arrow*). The highly enriched NPC fraction prior to HPLC is shown at the left (*NPCs*). Fractions 46–51 were pooled, separated by SDS-PAGE and transferred to PDVF membrane. The 100-kD band was excised, and then subjected to Lys-C cleavage and peptide sequence analysis. Peptide sequences derived from the polypeptide indicated in *A* were used to screen the GenBank/EMBL/DDBJ and SwissProt databases, identifying the open reading frame YKL057c (*B*). The deduced amino acid sequence is shown and is renamed Nup120p. The boxed sequences matched exactly with the peptide sequence derived from direct microsequencing with the exception of GLY-804 which could not be determined. Two putative leucine zippers and a third coiled–coil are underlined. A Blastp search of the yeast specific database revealed a similarity between Nup120p and Nup133p (*C*). Shown is the region of similarity (20% identity and 60% similarity) between the two proteins aligned by the FASTA program (Lipman and Pearson, 1985).

of the predicted double mutants failed to form colonies at 23°C. These results suggest synthetic lethality of the *NUP120* deletions with the four strains above.

Nuclear Pore Complexes Cluster in nup120Δ Cells

The characteristic punctate pattern of NPCs revealed by immunofluorescence microscopy using antibodies directed against NPC components represents the distribution of NPCs throughout the nuclear envelope. While this pattern is also observed with antibodies directed against the NPC marker protein Nup159p (Kraemer et al., 1995) in wild type cells, the NPCs of *nup120Δ* cells stained for this same marker were found clustered as a cap on one side of the nuclear envelope (Fig. 4). This was also the case for anti-Nsp1p antibodies (see below) and several other antibodies against NPC proteins (data not shown). The size and staining intensities of these capped structures varied markedly; indeed, some cells seemed to contain little, if any, staining material. Although most of the stained material in each cell was contained within the large cap, it was not infrequent for the remainder to be localized to one or more considerably smaller clusters located elsewhere on the nuclear envelope. This altered distribution was observed at both the semi-permissive temperature of 23°C and after the shift to 37°C, although after 6 h at the restrictive temperature the caps were often smaller and the cells contained less staining material overall (data not shown). Sim-

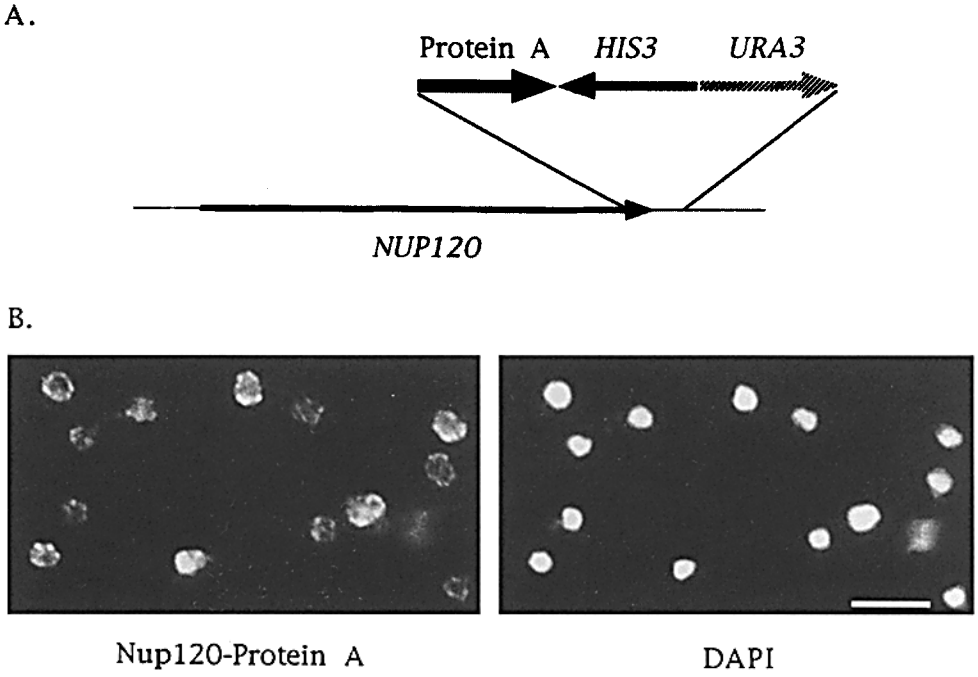

Figure 2. Immunofluorescent localization of Nup120p-protein A. Nup120 was tagged by an in-frame insertion of the IgG binding domains of protein A into the genomic *NUP120* gene generating a COOH-terminal fusion (*A*). The chimera was visualized in formaldehyde fixed yeast cells by affinity purified rabbit IgG followed by Cy3-labeled donkey anti-rabbit IgG revealing punctate nuclear rim staining characteristic of NPC-localization (*B*). The nuclear DNA was visualized by coincident staining with DAPI. Bar, 5 μm.

ilar staining has been observed with deletion of *NUP133* (Li et al., 1995; Doye et al., 1995; Pemberton et al., 1995), a temperature sensitive mutation of *NUP159* (Gorsch et al., 1995) and an amino terminal deletion of *NUP145* (Wente and Blobel, 1994).

To establish if the clustered NPCs were distributed randomly within the nuclear envelope, double immunofluorescent labeling was performed using mouse monoclonal antibodies directed against an abundant nucleolar protein Nop1p (Aris and Blobel, 1988) and rabbit polyclonal antibodies against Nsp1p (Nehrbass et al., 1990) (Fig. 5 *A*). The position of the NPC cap in each cell is marked in green,

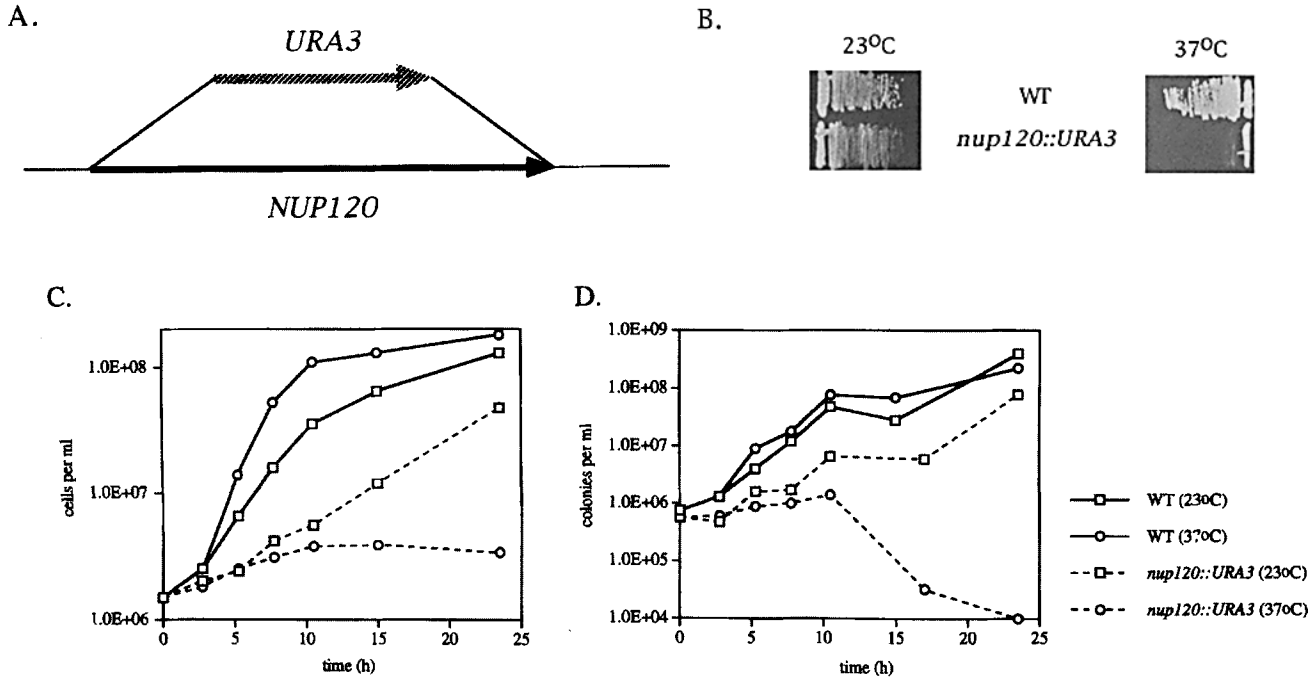

Figure 3. Deletion of *NUP120* results in temperature sensitivity, affecting growth rate and viability of *nup120Δ* cells. Deletion and disruption of the *NUP120* gene was accomplished by replacement of the *NUP120* ORF with the *URA3* selectable marker in the diploid strain DF5 (*A*). Heterozygous diploids containing a wild-type and a disrupted copy of *NUP120* were sporulated and tetrads dissected on YPD plates. While all four spores could be recovered, haploid cells carrying a disrupted copy of *NUP120* failed to grow at 37°C (*B*). *nup120Δ* cells (*nup120::URA3*) and haploid DF5 cells (*WT*) were grown in liquid medium at 23° and 37°C and were then counted at the indicated times (*C*). The number of viable cells was determined by plating aliquots of the cultures onto YPD and counting the colonies after 3 d at 23°C. *nup120Δ* cells failed to survive after one to two divisions at 37°C (*D*).

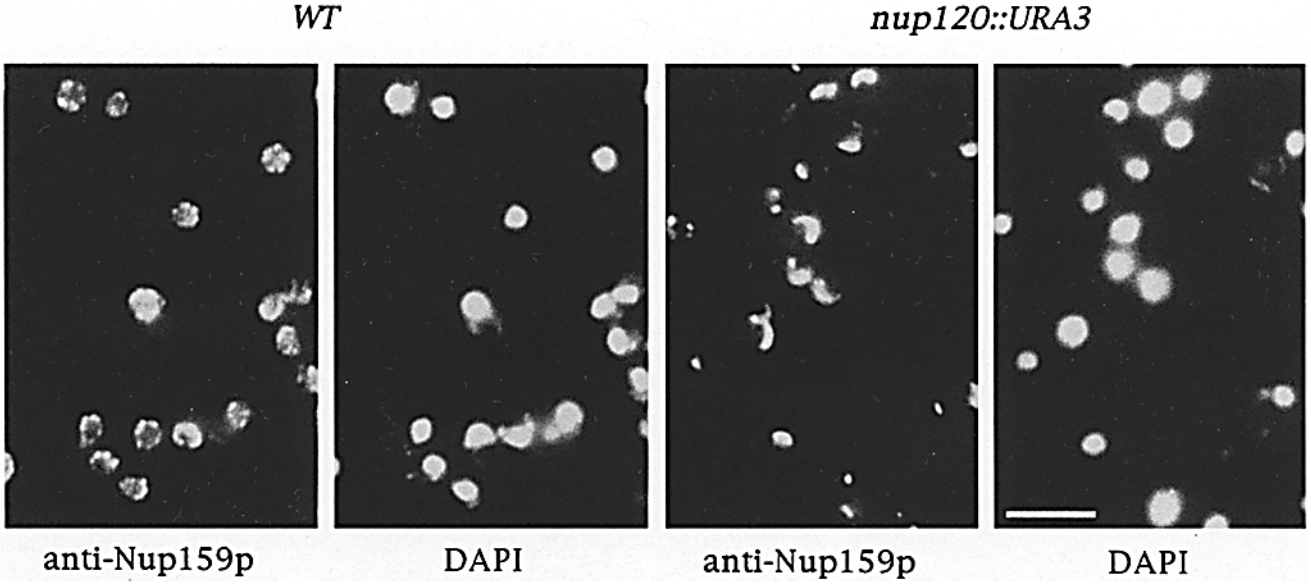

Figure 4. Nuclear pores cluster in *nup120Δ* cells. Examination of the NPCs of *nup120Δ* (*nup120::URA3*) and wild-type (*WT*) cells by immunofluorescence directed against the NPC marker protein Nup159p. NPCs are distributed throughout the nuclear envelope in wild-type cells whereas NPCs are clustered at one side of the nuclear envelope in *nup120Δ* cells at both the semi-permissive temperature 23°C and after the shift to 37°C (not shown). NPCs were visualized using the monoclonal antibody to Nup159p MAb165C10 (Kraemer et al., 1995) followed by Cy3-labeled donkey anti–mouse IgG. The nuclear DNA was visualized by coincident staining with DAPI. Bar, 5 μm.

whilst the nucleolus is red. Very few cells have coincident staining (*yellow*). These results indicate that the two structures generally occupy different regions of the nuclear envelope. In order to quantify this spatial arrangement, the orientation of the NPC cap was scored relative to the nucleolus by dividing the nuclear periphery into three areas: (*a*) opposite (~135°–225°); (*b*) adjacent (~45°–135° or ~225°–315°); and (*c*) coincident (~315°–45°) relative to the nucleolus (center at 0°) and analyzing overlaid fluorescent images. Since cells were oriented randomly, only cells where the crescent shape of the nucleolus (Aris and Blobel, 1988) could be clearly visualized were examined for the relative position of the NPC cap structure (Yang et al., 1989). In approximately 85% of the cells the NPC cap structure was oriented opposite to the nucleolus, whereas less than 3% of the cells showed coincident nucleolar and NPC staining (Fig. 5 *B*). Even this apparent coincidence may be explained by the orientation of the nucleus, such that the nucleolus lies directly above or below (though still separate from) the NPC cluster. These results suggest that the orientation of the clustered NPCs is not random and may reflect a higher order structure within the nucleus.

Effect of NUP120 Deletion on Nuclear Markers

In order to determine whether the deletion of *NUP120* affected nuclear structures other than the nuclear envelope, we compared the distribution of different nuclear markers by immunofluorescence microscopy in *nup120Δ* cells and wild-type cells at various times after a shift to the restrictive temperature. The most striking observation was that of a progressive disintegration of nucleolar morphology after the temperature shift in *nup120Δ* cells, as visualized with a monoclonal antibody against Nop1p (Aris and Blobel, 1988). In wild-type cells, nucleoli stained with this antibody appear as crescent-shaped structures, faintly lobulated, and with their convex surface tightly apposed to the inner face of the nuclear envelope (Fig. 6 *A*). This morphology was found to be similar at all time points after the temperature shift. In contrast, the nucleoli of *nup120Δ* cells were slightly abnormal even at the semi-permissive temperature (Fig. 6 *A*).

Approximately 20% of the cells showed some signs of nucleolar fragmentation, which was usually manifested as one or two small, spherical patches of staining near a nucleolus of approximately normal size and appearance. However, after 1 h, there was a dramatic increase in the proportion of fragmented nucleoli. Over 70% of the cells contained the spherical patches, which were larger and could number as many as five per cell. Nucleoli, if distinguishable, appeared to be more diffuse and less sharply associated with the nuclear envelope. This phenotype had become slightly more pronounced by 3 h (Fig. 6 *A*). By this time point, most of the nucleoli were smaller, and some were difficult to locate at all. The overall intensity of staining was lower than for comparable wild-type cells, or mutant cells at the semi-permissive temperature. After 6 h, a normal nucleolus could be found in only a few cells, the rest carrying numerous spherical patches of varying size and intensity (data not shown). Nucleolar dispersal made it impossible to correlate the position of the capped NPCs with the nucleolus at the restrictive temperatures. This nucleolar fragmentation was also observed by thin-section electron microscopy (Fig. 6 *B*). At the semi-permissive temperature, each nucleolus appeared as a single denser region of chromatin appressed to the nuclear envelope and opposite the clustered NPCs (Fig. 6 *B*, *arrows*). After 3 h at the restrictive temperature, the nuclei of many cells

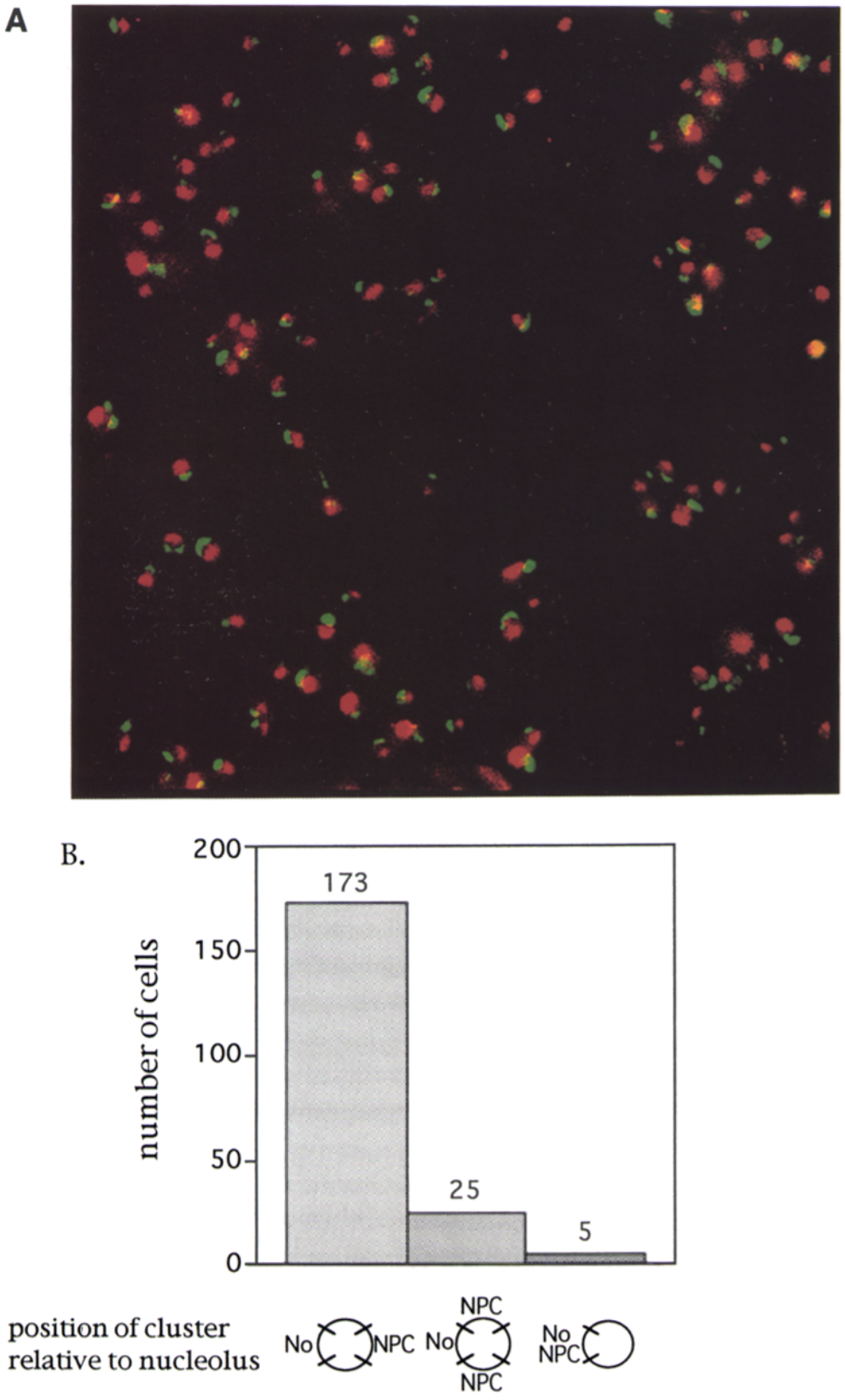

Figure 5. Double-labeled immunofluorescent staining of *nup120Δ* cells, showing that the NPC (*green*) were generally opposite the nucleoli (*red*) (*A*). The image is a computer generated composite from a single field of cells double labeled with a rabbit polyclonal anti-Nsp1p antibody (NPC protein; *green*) (EC10-2; Hurt, 1988) visualized with a fluorescein-conjugated donkey polyclonal anti-rabbit IgG antibody, and a monoclonal anti-Nop1p antibody (D77; Aris and Blobel, 1988) visualized with a Cy3-conjugated polyclonal donkey anti-mouse IgG antibody (nucleolar protein; *red*). The orientation of the NPC cap (*NPC*) in each cell was scored relative to the nucleolar position (*No*) (*B*) for a total of 200 cells. The relative orientations were divided into three classes as shown schematically: (*a*) opposite (~135°–225°); (*b*) adjacent (~45°–135° or ~225°–315°); and (*c*) coincident (~315°–45°) relative to the nucleolus (center at 0°). The histogram shows the number of cells in each class.

contained several denser regions of chromatin, most being circular in section and detached from the nuclear envelope, spread throughout the nucleoplasm (Fig. 6 *B*, *arrows*).

The spindle was another nuclear marker whose structure became markedly altered as a result of the temperature shift. Measurements of spindle lengths in normal haploid yeast cells either 0 or 3 h after the shift to the restrictive temperature showed a broadly bimodal distribution; though the majority of spindles were between 0.5–1.5-μm long, representing cells in G1, S, and G2 phases of the cell cycle,

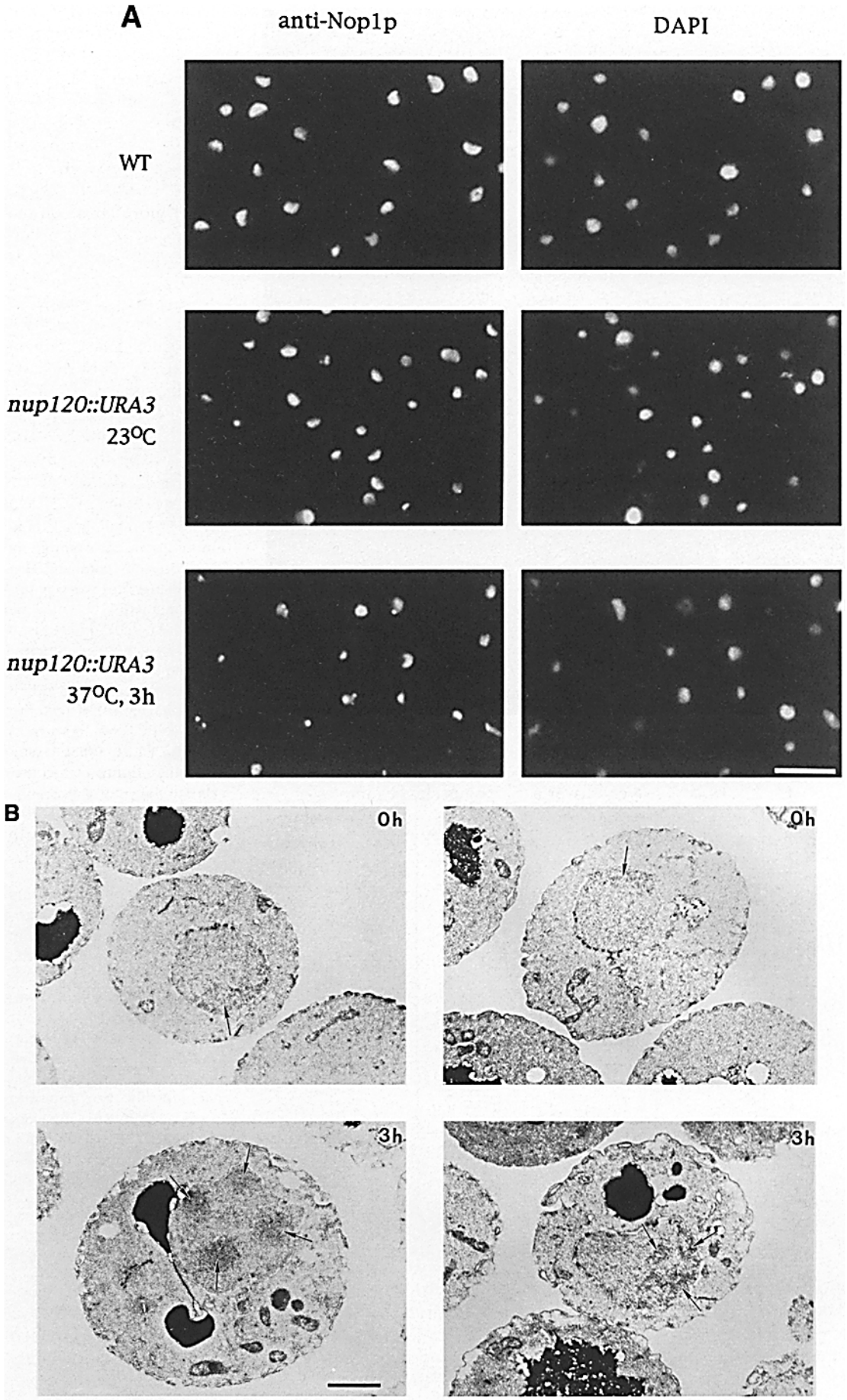
A
anti-Nop1p
DAPI
WT
nup120::URA3
23°C
nup120::URA3
37°C, 3h
B
0h
0h
3h
3h

a minority (~20%) were much longer, between 3.0–6.0 μm, displaying cells between G2 and the end of M (Fig. 7; Byers and Goetsch, 1975; Winey et al., 1995). In contrast, *nup120Δ* cells appeared to be defective in their ability to properly form extended spindles even under semi-permissive conditions (which may reflect their longer doubling time) (Fig. 7). After 3 h at the restrictive temperature, only 3% of the spindles in *nup120Δ* cells exceeded 2.5 μm, compared with 23% in normal cells. Microtubule morphology in these cells was also abnormal; many cells contained unusually long cytoplasmic microtubules, and in some cells two clear, separate foci of microtubules could be seen, as if the spindle pole bodies had separated without forming a full spindle (Fig. 7). The frequency of budded cells in this population was also slightly higher than normal. These observations would suggest that the restriction causes a specious mitotic defect. A similar effect has been noted for a conditional mutation of the nuclear import receptor, *SRP1* (*KAP60*) (Loeb et al., 1995).

The effect of the temperature shift on the distribution of another nuclear marker, Nsr1p (Lee et al., 1991) was less obvious, although that proportion of the protein associated with the nucleoli reflected the progressive fragmentation observed with Nop1p, demonstrating that the phenomenon was not restricted to this marker, but was more likely a general effect on nucleolar architecture. Likewise, the distribution of chromatin within the nucleus did not seem grossly changed over the course of the temperature shift in the *nup120Δ* cells, as determined by DAPI staining (Figs. 6 *A*, 9, and 10).

Morphological Examination of nup120Δ Cells

The gross phenotypic effects of deletion of *NUP120*, as described above, are readily observed at the level of the light microscope. We therefore examined *nup120Δ* cells over a period of several hours following a shift to the restrictive temperature by thin-section electron microscopy in order to detect more subtle changes to the cellular ultrastructure. At the start of the shift, when the cells still exhibit their semi-permissive phenotype, the most striking morphological perturbations were the clusters of NPCs. These clustered structures were characterized by large islands of closely opposed NPCs spaced by short highly distorted regions of nuclear envelope (Fig. 8, *0h*, *arrows*). However, in common with *nup159ts* mutant cells (Gorsch et al., 1995), *nup145ΔN* cells (Wente and Blobel, 1994), and *nup133Δ* cells (Li et al., 1995), NPCs could occasionally be found outside the clusters in apparently normal regions of the nuclear envelope (Fig. 8, *0h*, *arrowheads*). One unique feature of *nup120Δ* cells was the degree of distortion of the spacer nuclear envelope in the NPC clustered regions, which was more extreme than that seen with either the *nup159* or *nup133* mutants but considerably less so than the *nup145* mutant. Occasional small aggregates of electron dense material were also detected in the nucleoplasm (Fig. 8, *a*). After 3 h at the restrictive temperature, the clusters had evolved into a more elaborate lattice of cisternae and herniations interconnected by NPCs. These now strongly resembled the grape-like structures described for the *nup145ΔN* cells (Wente and Blobel, 1994). Like these, some very large herniations could be seen over one or more NPCs on the cytoplasmic side of the clusters (Fig. 8, *3h*, *arrows*). Herniations were also seen in *nup116Δ* cells, forming a seal over the cytoplasmic face of the NPC (Wente and Blobel, 1992). The *nup116Δ* herniations were filled with an electron dense material which, by virtue of a peripheral punctate oligo(dT) fluorescence staining pattern seen in this same strain of cells, was identified as ribonucleoprotein. This was believed to have accumulated as a result of nuclear export through the NPC, filling the herniation with electron dense ribonucleoproteins. However, neither the *nup120Δ* nor the *nup145ΔN* herniations were filled with electron dense material, and at least in the case of the *nup120Δ* cells no peripheral punctate oligo(dT) staining was detected (see below). This may be due to the fact that NPCs could be found interconnecting the cluster's cisternae and on their cytoplasmic faces, allowing the exchange of the cisternal contents with both the nucleoplasm and cytoplasm. Occasionally, adjacent nuclear membrane protuberances could be found curving towards each other (Fig. 8, *3h*, *arrowheads*). It is possible that these were in the process of joining to form another cisterna, as proposed for the mechanism of herniation formation in the *nup116Δ* mutant. At 6 h the cells exhibited comparable or more extreme versions of the structures found at 3 h (some of the herniations were particularly large; Fig. 8, *6h*, *arrow*), and at both time points clear examples of electron dense areas of the nucleoplasm could be seen. Similar aggregates of material in the nucleoplasm have been reported for the *nup116Δ* cells (Wente and Blobel, 1993) and for various RNA export mutants (Schneiter et al., 1995).

Nuclear Transport at Restrictive Temperatures in nup120Δ Cells

Analysis of the distribution of poly(A)$^+$ RNA in situ in *nup120Δ* was investigated using digoxigenin-labeled oligo(dT)$_{30}$ followed by FITC-labeled anti-digoxigenin antibodies. There was no detectable accumulation of poly(A)$^+$ RNA in the nucleus of *nup120Δ* cells at the semi-permissive temperature (23°C) or in wild-type cells at either 23° or 37°C. However within 1 h after the shift of *nup120Δ* cells to the restrictive temperature (37°C), poly(A)$^+$ RNA

Figure 6. Nucleoli fragment in *nup120Δ* cells. Examination of the nucleoli of *nup120Δ* (*nup120::URA3*) and wild-type (*WT*) cells by immunofluorescence directed against the nucleolar marker protein Nop1p (*A*). Nucleoli are intact, crescent shaped, and lie against the nuclear envelope in wild-type cells whereas they are fragmented to a moderate extent at permissive temperature (23°C) and to a much greater extent after a shift to the restrictive temperature (37°C) for 3 h. Nucleoli were visualized using the monoclonal antibody to Nop1p followed by Cy3-labeled donkey anti–mouse IgG. The nuclear DNA was visualized by coincident staining with DAPI. Electron micrographs (*B*) showing the relatively normal appearance of the nucleoli (*0h*, *arrows*) opposite the NPC clusters in *nup120Δ* cells at the semi-permissive temperature. After 3 h at the restrictive temperature, the nucleoli have clearly fragmented (*3h*, *arrows*). Bars: (*A*) 5 μm; (*B*) 1 μm.

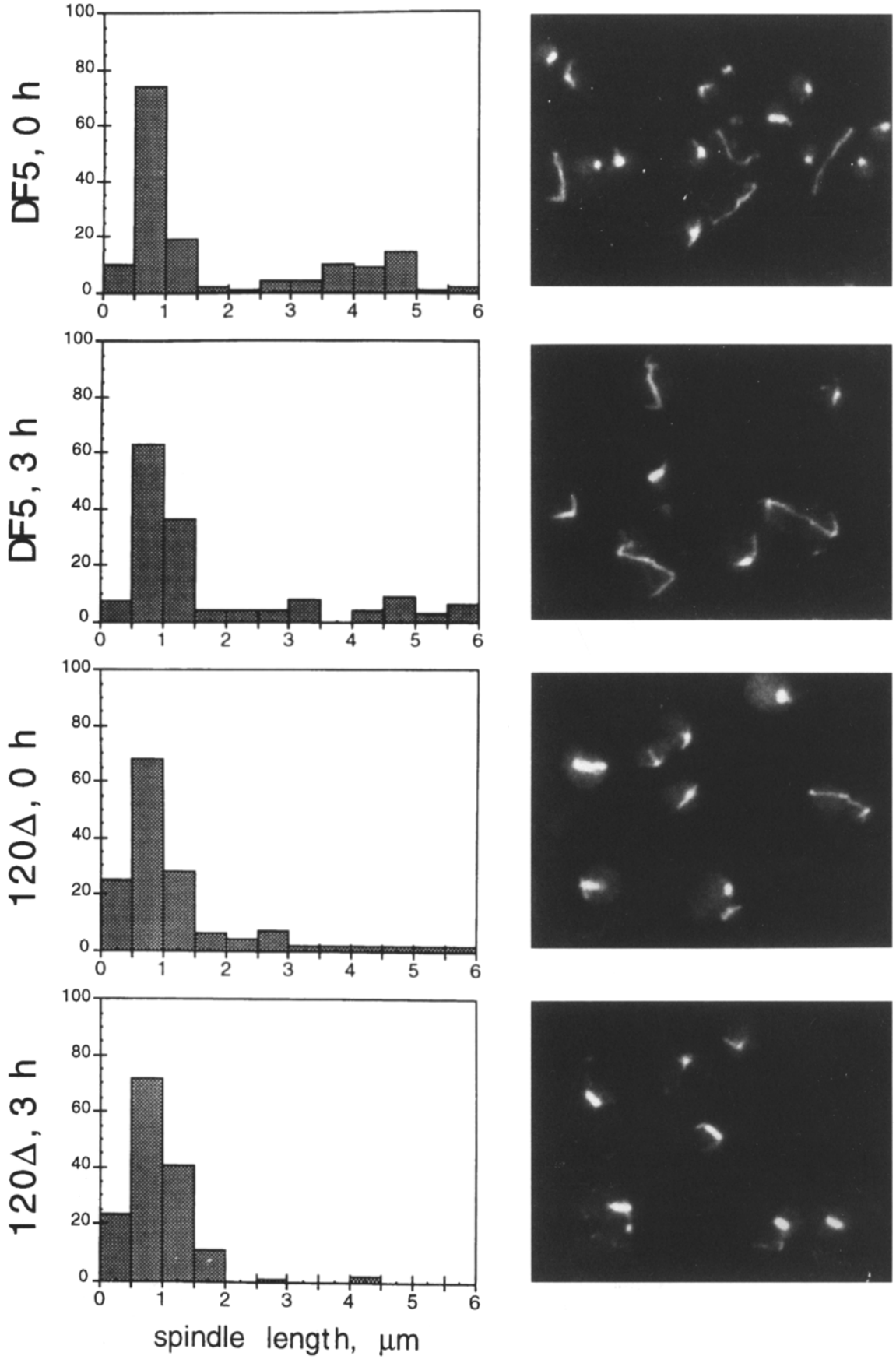
DF5, 0 h
DF5, 3 h
120Δ, 0 h
120Δ, 3 h
100
80
60
40
20
0
0 1 2 3 4 5 6
spindle length, μm

began to accumulate within the nucleus of some cells, and by 3 and 6 h, most of the cells displayed the poly(A)$^+$ RNA export block (Fig. 9). The immunofluorescent signal was not localized to the periphery of the nucleus as observed for *nup116Δ* cells (Wente and Blobel, 1993) indicating that the mRNA does not accumulate in herniations of the nuclear envelope. The accumulation of poly(A)$^+$ RNA may be the primary effect leading to cell death in these cells as it occurs before the cells have stopped dividing and die (see Fig. 3).

Attempts to investigate the effect of nuclear import after the temperature shift failed to yield conclusive results. Using the nuclear protein Nsr1p as a marker (Lee et al., 1991) we could detect very little cytoplasmic accumulation of the immunofluorescent signal in *nup120Δ* cells as compared to wild-type cells after the shift to 37°C (data not shown). We therefore investigated the effects of temperature shift on the distribution of the shuttling import factor Kap60p (SRP1p) (Yano et al., 1992; Enenkel et al., 1995; Moroianu et al., 1995*a*). Although it has not been demonstrated in yeast, the mammalian homologue of Kap60p, karyopherin α, has been shown to be imported into the nucleus coincident with the import of substrate and to shuttle out of the nucleus, presumably for the next round of import (Moroianu et al., 1995*b*; Görlich et al., 1995; Moroianu, J., and G. Blobel, unpublished observation). Indirect immunofluorescence microscopy using anti-Kap60p antibodies showed a distinct nuclear accumulation in *nup120Δ* cells after the temperature shift compared to wild-type cells where the protein, under the fixation conditions used here, appeared equally distributed between the nucleus and the cytoplasm (Fig. 10). The accumulation of Kap60p and poly(A)$^+$ RNA in the nucleus, combined with only a moderate effect on Nsr1p cytoplasmic accumulation is consistent with the idea that protein import remains relatively unaffected by the the temperature shift, but that export of mRNA and Kap60p is significantly hindered.

Discussion

We have identified a novel nucleoporin we term Nup120p. This protein shows limited homology to Nup133p and no significant similarity to any other proteins in the data base. Nup120p (and its corresponding ORF, YKL057c) was identified by microsequence analysis of a protein ($M_r \sim 100{,}000$) present in a yeast subcellular fraction highly enriched in NPCs. Nup120p is present in this fraction in similar amounts to Nup133p (Rout and Blobel, 1993; Pemberton et al., 1995), but is not as abundant as Nic96p, Nup170p, Nup157p, Nup188p, or Pom152p (Aitchison et al., 1995). Immunofluorescent localization of a protein A–tagged Nup120p chimera and subcellular fractionation demonstrate that the protein is localized to the NPC. Furthermore, deletion of *NUP120* causes a temperature sensitive block in poly(A)$^+$ RNA export, a wide spectrum of coincident morphological defects and constitutive NPC clustering. It is also synthetically lethal in combination with deletion of the genes encoding *NUP170*, *NUP188*, *POM152*, and *NUP133*.

The nuclear accumulation of poly(A)$^+$ RNA has been reported for mutations in the genes of several nucleoporins: *NUP159* (Gorsch et al., 1995), *NUP145* (Wente and Blobel, 1994), *NUP133* (Li et al., 1995), *NUP116* (Wente and Blobel, 1993), and *NUP82* (Hurwitz and Blobel, 1995). This is likely to be the primary cause of the temperature-sensitive phenotype of *nup120Δ* cells, as there were no accompanying detectable nuclear import defects. Of course, the failure to detect cytoplasmic accumulation of endogenous nuclear proteins is not necessarily indicative of efficient nuclear import because mRNA export precedes protein synthesis. However, the accumulation of Kap60p (SRP1) in the nucleus after the temperature shift, coincident with the poly(A)$^+$ RNA export defect, suggests that the NPCs maintain import capabilities but have become export deficient. The RNA export defect may itself lead to several other pleiotropic effects on the morphology of the nucleus, although no obvious morphological phenotypes were coincident with a poly(A)$^+$ RNA export defect in *nup82* cells (Hurwitz and Blobel, 1995).

Nucleolar fragmentation and dissociation from the nuclear envelope, although not reported for alterations in nucleoporins, has been observed in several RNA export mutants (reviewed in Schneiter et al., 1995) and may be a result of poly(A)$^+$ RNA accumulation (Kadowaki et al., 1994). Thus it is not surprising that an NPC protein whose loss causes a defect in poly(A)$^+$ RNA export may also cause nucleolar fragmentation. The structure of the nucleolus may be dynamically maintained by a balance in the nuclear import of material required for pre-ribosomal assembly and the export of pre-ribosomes and mRNAs required for component synthesis. Also, as discussed by Schneiter et al. (1995), the nucleolus itself may be involved in poly(A)$^+$ RNA export.

Abnormal spindle function as a potential consequence of defective nucleocytoplasmic transport has been reported for one other NPC-associated protein, namely the nuclear import factor Srp1p (Kap60p) (Loeb et al., 1995). This also resulted in an apparent mitotic defect, similar to that seen in *nup120Δ* cells at the restrictive temperature. Loeb et al. (1995) presented evidence that this defect was caused by an inability to import factors necessary for the degradation of key mitotic regulators, such as Clb2p. It is also possible that inefficient export of RNAs encoding other mitotically required proteins, such as MAPs and motor proteins, in turn causes the rapid cessation of cell division after the temperature shift.

The most dramatic morphological defect associated with the deletion of the *NUP120* gene is NPC clustering. NPC clustering has also been reported for mutations in *NUP145*

Figure 7. Effect on the spindle morphology of wild-type and *nup120Δ* cells after 3 h at the restrictive temperature. (*Left*) Histogram of 150 spindle lengths measured for each cell population. (*Right*) Representative immunofluorescent labeling of the spindles in a number of cells in each population, using a polyclonal antibody against yeast tubulin visualized with a Cy3-conjugated polyclonal anti–rabbit IgG antibody. Wild-type cells display a normal population of spindle lengths at both the semi-permissive temperature (*DF5, 0 h*) and after 3 h at the restrictive temperature (*DF5, 3 h*). In contrast, *nup120Δ* cells have somewhat defective spindles at the semi-permissive temperature (*120Δ, 0 h*) and appear unable to make long spindles after 3 h at the restrictive temperature (*120Δ, 3 h*).

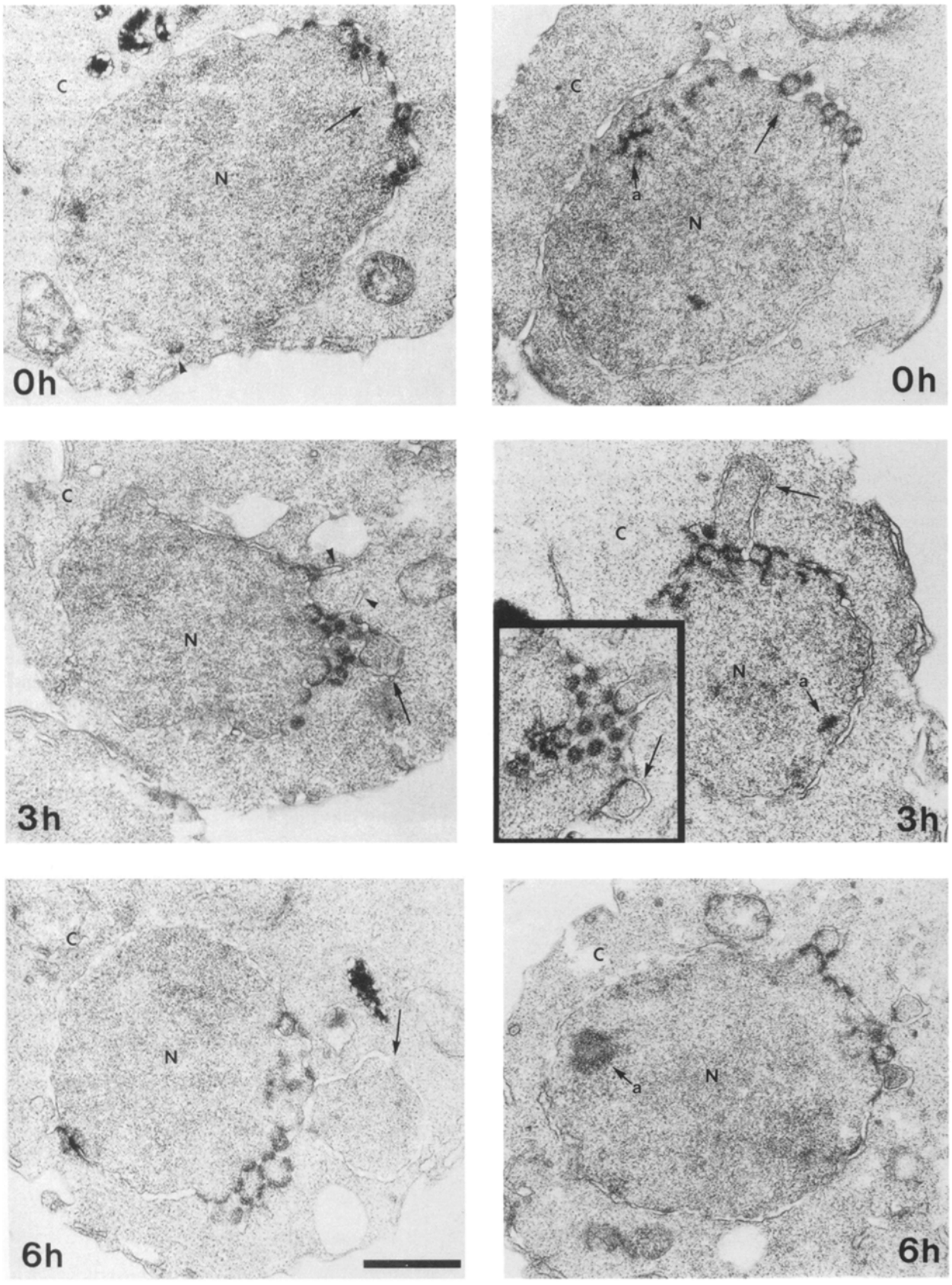

Figure 8. Electron micrographs of *nup120Δ* (*nup120::URA3*) cells at the permissive temperature (23°C) (*0h*) and after a shift to the restrictive temperature (37°C) for 3 and 6 h. The micrographs depict NPC clustering at both temperatures. At 23°C the clustered structures were characterized by large islands of closely opposed NPCs spaced by short highly distorted regions of nuclear envelope (*0h*, *arrows*); occasionally, isolated NPCs were also seen (*0h*, *arrowheads*). There is a great degree of distortion of the spacer nuclear envelope

(Wente and Blobel, 1994), *NUP133* (Doye et al., 1995; Li et al., 1995; Pemberton et al., 1995), and *NUP159* (Gorsch et al., 1995). It is interesting to note that it is the region of Nup133p whose removal causes NPC clustering in *nup133* cells that is most similar to a stretch in Nup120p. It has yet to be determined whether this homologous region on Nup120p is also responsible for maintaining the spatial distribution of NPCs in the nuclear envelope.

NPC clustering as a result of the loss of Nup120p occurs at both the semi-permissive and restrictive temperatures and is not linked to the observed transport defect. Demonstration that the clustering phenomenon does not itself cause cell death has also been shown for each of the other reported clustering mutants (Wente and Blobel, 1994; Doye et al., 1995; Gorsch et al., 1995). The morphological abnormalities associated with clustered NPCs observed here after a temperature shift of *nup120Δ* cells most closely resemble the grape-like clusters reported in *nup145ΔN* cells (Wente and Blobel, 1994). In both these strains, there are extensive nuclear envelope protrusions in the region of the NPC clusters. These clusters and envelope abnormalities in cells lacking Nup120p may reflect, as suggested by Wente and Blobel (1994), a disturbed connection of mutant NPCs with the pore membrane domain of the nuclear envelope, thus allowing fusion of the nuclear envelope over assembling NPCs. Not exclusive to this possibility is that NPC clustering may reflect a breakdown of NPC interaction with the nuclear or cytoskeletal matrix. As NPCs in wild-type cells are evenly distributed over the entire nuclear envelope (including that portion attached to the nucleolus), a uniform NPC distribution may be normally actively organized and maintained. This is supported by the extraordinary organization of NPCs found in cells from several higher eukaryotes including *Xenopus*, *Equisetum*, and *Necturus* (Maul, 1977; Akey, 1989). Loss of an NPC component disrupting this interaction (directly or indirectly) could therefore cause clusters of NPCs. The finding that NPC clusters in *nup120Δ* cells are generally found opposite the nucleolus may reflect the collapse of a higher order nuclear structure and diffusion of NPCs to a particular focal point in the nuclear envelope. Comparably, NPCs of spermatozoan nuclei are found clustered to one pole of the nuclear envelope in areas where the heterochromatin loops touch the nuclear envelope (Fawcett, 1981). It is unknown whether this structure is actively maintained or is a result of a lack of complex chromatin structure or nuclear matrix organization. Alternatively, the dynamics of the nuclear envelope itself could be affected by an altered structure of the pore membrane domain. This domain is believed to be the sole exchange site of membrane components between the inner and outer nuclear membranes and itself is tightly surrounded by NPC proteins (Akey and Rademacher, 1993; Wozniak et al., 1994). Perturbations in proteins surrounding or associated with this domain may in turn affect both its structure and the efficient exchange of materials between the two membranes. Thus, the clustering phenomenon may result from an alteration of the inner nuclear membrane composition (or lamina) or the local membrane environment surrounding each NPC.

It is curious that mutations in apparently dissimilar NPC components can lead to common morphological abnormalities, some of which are shared by *nup120*. So far, these would seem to fall into at least four broad classes, although obviously some overlap occurs. The first group includes genes which cause NPC clustering and ultimately the grape-like structures, as described here for *nup120*, are also observed in *nup145* and *nup133* cells. The second, seen in *nup1* mutants and in various synthetic lethal combinations of *nup170*, *nup188*, and *pom152*, typically has cells with extreme convolutions and invaginations of the nuclear envelope, carrying seemingly normally spaced NPCs (Belanger et al., 1994; Aitchison et al., 1995; Nehrbass, U., S. Maguire, M. P. Rout, G. Blobel, and R. W. Wozniak, manuscript submitted). The third, displaying herniations which contain electron dense material over the cytoplasmic face of NPCs, is at the moment unique to *nup116* cells. The fourth, like *nup82*, or individual deletions of *NUP157*, *NUP170* (Aitchison et al., 1995), *NUP188* (Nehrbass, U., S. Maguire, M. P. Rout, G. Blobel, and R. W. Wozniak, manuscript submitted), and *POM152* (Wozniak et al., 1994), has no discernible structural phenotype.

The relatively distinct phenotypic classes described above would argue against the idea that their morphologies are the result of a pleiotropic effect caused by a general nuclear transport defect. It is not clear why the alteration or removal of such disparate proteins should cause these common phenotypes; perhaps those with similar phenotypes are components recruited at the same time in the sequential assembly of new NPCs, or are separate components of an NPC subcomplex with a defined set of functions, or affect the transport efficiencies of a subset of substrates. Alteration or removal of one component could lead to a failure in that step of NPC assembly, or produce a functionally compromised subcomplex. Either (or both) scenarios could in turn produce characteristic morphological perturbations, common to a particular pathway of assembly or transport. Furthermore, the severity of the morphological disturbances does not necessarily correlate with the cell viability. For example, the *nup145ΔN* mutant, with extreme convolutions of the nucleus, is relatively healthy; whereas the depletion of Nup82p causes no detectable morphological phenotype, but is lethal (Wente and Blobel, 1994; Hurwitz and Blobel, 1995).

The synthetic lethality caused by combination of *nup120Δ* with single deletions of *NUP170*, *NUP188*, or *POM152* suggests a relatively specific genetic interaction. This does not imply direct physical interactions or overlap in the specific functions of these proteins, but may simply be a result

in the NPC clustered regions. Occasional small aggregates of electron dense material (*a*) were also detected in the nucleoplasm. After 3 h at 37°C, the clusters had evolved into a more elaborate lattice of cisternae and herniations interconnected by NPCs. Like these, some very large herniations could be seen over one or more NPCs on the cytoplasmic side of the clusters (*3h*, *arrows*). Protrusions apparently caught in the act of joining were sometimes found (*3h*, *arrowheads*). After 6 h at 37°C the cells exhibited comparable or more extreme versions of the structures found at 3 h (some of the herniations were particularly large; *6h*, *arrow*), and at both time points clear examples of electron dense areas of the nucleoplasm (*a*) could be seen. Bar, 0.5 μm.

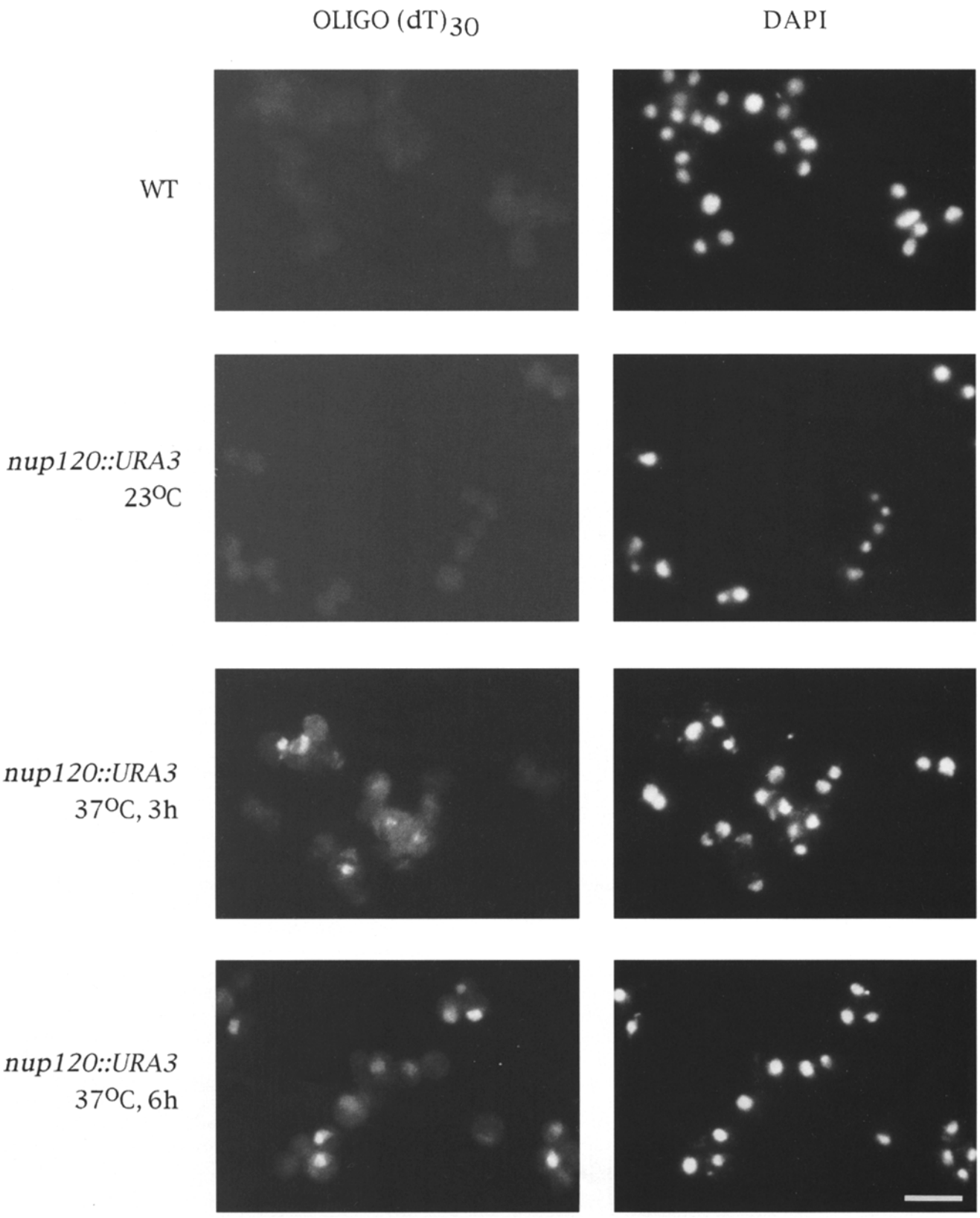

Figure 9. Poly(A)$^+$ RNA accumulates in the nucleus of *nup120Δ* cells. In situ hybridization of oligo(dT)$_{30}$ in *nup120Δ* cells (*nup120::URA3*) showed accumulation of poly(A)$^+$ RNA within the nucleus upon shift to the restrictive temperature, compared to wild-type cells (*WT*). The accumulation of poly(A)$^+$ RNA may be the primary effect leading to cell death in these cells as it occurs before the cells have stopped dividing and die (see Fig. 3). The digoxigenin-labeled oligo(dT)$_{30}$ was detected using fluorescein-conjugated antidigoxigenin antibodies. DAPI shows coincident staining of nuclear DNA. Bar, 5 μm.

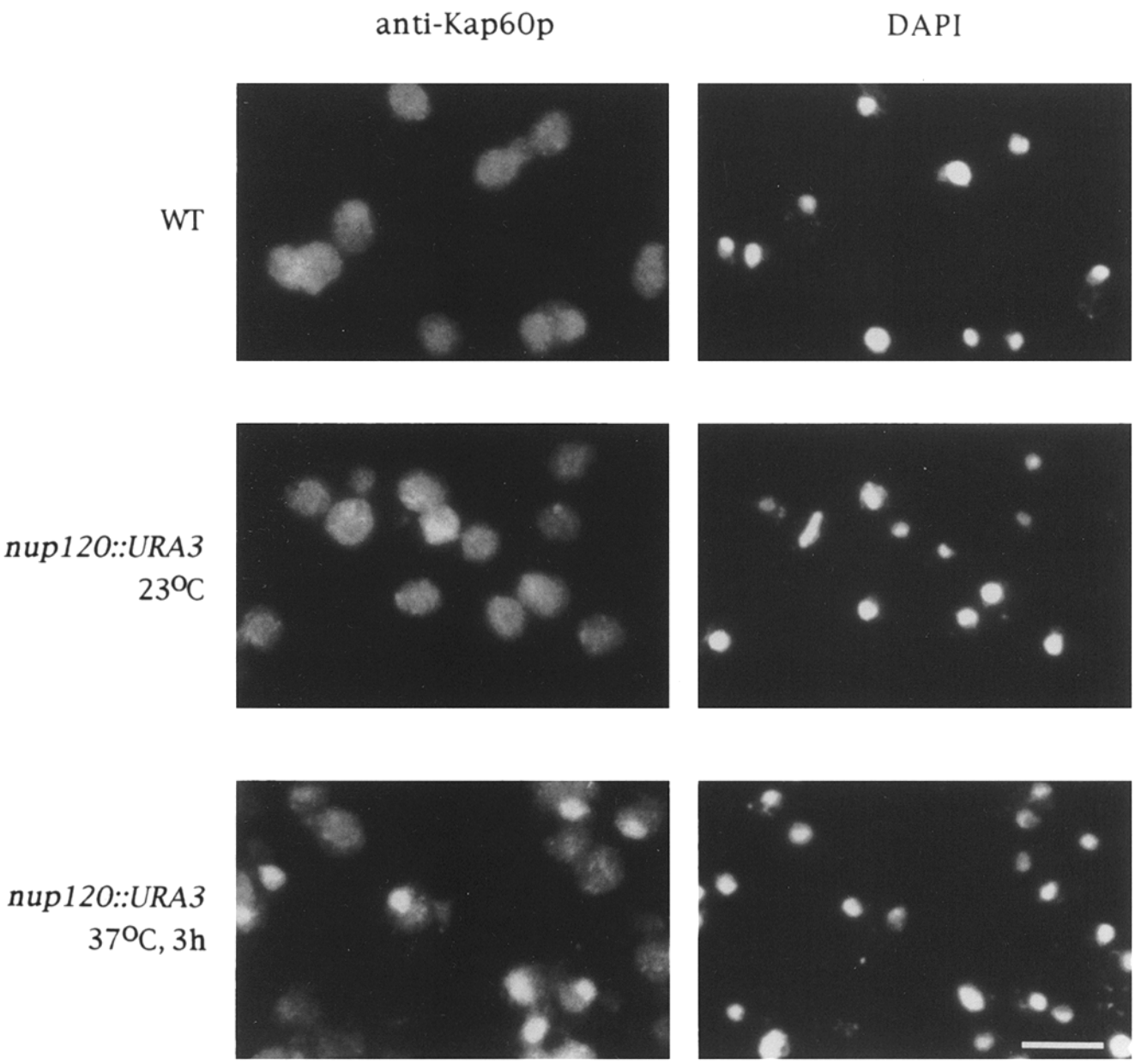

Figure 10. The transport factor karyopherin α (Kap60p, SRP1) accumulates in the nucleus of *nup120Δ* cells (*nup120::URA3*), compared to wild-type cells (*WT*). Under these fixation conditions Kap60p is detected by immunofluorescence in the nucleus and cytoplasm of wild-type (*WT*) cells reflecting its shuttling between the nucleus and cytoplasm. Examination of (*nup120::URA3*) revealed similar distribution at permissive temperature (23°C) but Kap60p accumulation in the nucleus after a shift to the restrictive temperature (37°C) for 3 h. Kap60p was visualized using rabbit IgG antibody followed by Cy3-labeled donkey anti–rabbit IgG. DAPI shows coincident staining of nuclear DNA. Bar, 5 μm.

of their presence in, and contributions to, the overall structure of the NPC. We assume that deletion of *NUP120* compromises the structural integrity of the NPC resulting in the temperature sensitivity of *nup120Δ* cells and the associated phenotypes. Combining this defect with deletions of other nucleoporins, whether or not they themselves show an obvious phenotype, may further jeopardize the integrity of the NPC leading to its collapse. The situation becomes more difficult to interpret with the combination of *nup120Δ* with *nup133Δ*, since deletion of either on its own is deleterious to cell growth and viability. This synthetic lethal combination could equally be attributed to a combined effect on overall cell fitness, i.e., a result of the sick getting sicker. Because the NPC is a compact and complex organelle, with each NPC component likely interacting with many other NPC components (either indirectly or directly) to form the functional whole, numerous combinatorial synthetic lethal interactions would be expected. Therefore, such genetic interactions should not be overinterpreted in terms of the specific function of each nucleoporin.

The removal of Nup120p from the yeast NPC has extensive and varied effects on the nuclear morphology and function, which ultimately compromise cell growth and viability. As well as underscoring the intimate role NPCs play in

the active maintenance of eukaryotic cells, these results provide avenues to pursue concerning the interplay of apparently disparate processes in the cell life cycle.

We thank The Rockefeller University/Howard Hughes Medical Institute Biopolymer Facility for oligonucleotide synthesis and peptide sequencing, especially Joseph Fernandez; Eleana Sphicas for assistance in performing the electron microscopy studies; Drs. Ulf Nehrbass, Felix Kessler, and Mark Winey for helpful discussions; Dr. Lucy Pemberton for providing the *nup133* strain; Dr. John Kilmartin for anti-Nsrlp and anti-tubulin antibodies; Dr. Ed Hurt for anti-Nspl antibodies; and the Nomura Laboratory for anti-SRP1 antibodies. J. D. Aitchison is a Medical Research Council of Canada Postdoctoral Fellow.

Received for publication 6 September 1995 and in revised form 13 October 1995.

References

Aitchison, J. D., M. P. Rout, M. Marelli, G. Blobel, and R. W. Wozniak. 1995. Two novel related yeast nucleoporins Nup170p and Nup157p: complementation with the vertebrate homologue Nup155p and functional interactions with the yeast nuclear pore-membrane protein Pom152p. *J. Cell Biol.* 131: 1133–1148.

Akey, C. W. 1989. Interactions and structure of the nuclear pore complex revealed by cryo-electron microscopy. *J. Cell Biol.* 109:955–970.

Akey, C. W., and M. Radermacher. 1993. Architecture of the *Xenopus* nuclear pore complex revealed by three-dimensional cryo-electron microscopy. *J. Cell Biol.* 122:1–19.

Alber, T. 1992. Structure of the leucine zipper. *Curr. Opin. Genet. Dev.* 2:205–210.

Aris, J. P., and G. Blobel. 1988. Identification and characterization of a yeast nucleolar protein that is similar to a rat liver nucleolar protein. *J. Cell Biol.* 107:17–31.

Belanger, K. D., M. A. Kenna, S. Wei, and L. I. Davis. 1994. Genetic and physical interactions between Srp1p and nuclear pore complex proteins Nup1p and Nup2p. *J. Cell Biol.* 126:619–630.

Byers, B., and L. Goetsch. 1975. Behavior of spindles and spindle plaques in the cell cycle and conjugation of *Saccharomyces cerevisiae*. *J. Bacteriol.* 124:511–523.

Byrd, D. A., D. J. Sweet, N. Pante, K. N. Konstantinov, T. Guan, A. C. S. Saphire, P. J. Mitchell, C. S. Cooper, U. Aebi, and L. Gerace. 1994. Tpr, a large coiled coil protein whose amino terminus is involved in activation of oncogenic kinases, is localized to the cytoplasmic surface of the nuclear pore complex. *J. Cell Biol.* 127:1515–1526.

Delorme, E. 1989. Transformation of *Saccharomyces cerevisiae* by electroporation. *Appl. Environ. Microbiol.* 55:2242–2246.

Doye, V., R. Wepf, and E. C. Hurt. 1994. A novel nuclear pore protein Nup133p with distinct roles in poly(A)$^+$ RNA transport and nuclear pore distribution. *EMBO J.* 13:6062–6075.

Enenkel, C., G. Blobel, and M. Rexach. 1995. Identification of a yeast karyopherin heterodimer that targets import substrate to mammalian nuclear pore complexes. *J. Biol. Chem.* 270:16499–16502.

Fabre, E., and E. C. Hurt. 1994. Nuclear transport. *Curr. Opin. Cell Biol.* 6:335–342.

Fawcett, D. W. 1981. The Cell. W. B. Saunders Company, Philadelphia London Toronto.

Fernandez, J., L. Andrews, and S. M. Mische. 1994. An improved procedure for enzymatic digestion of polyvinyldiene difluoride-bound proteins for internal sequence analysis. *Anal. Biochem.* 218:112–117.

Forrester, W., F. Stutz, M. Rosbash, and M. Wickens. 1992. Defects in mRNA 3′-end formation, transcription initiation, and mRNA transport associated with the yeast mutation prp20: possible coupling of mRNA processing and chromatin structure. *Genes & Dev.* 6:1914–1926.

Fuchs, R. 1991. MacPattern: protein pattern searching on the Apple Macintosh. *Comp. Appl. Biosci.* 7:105–106.

Gerace, L., Y. Ottaviano, and K. C. Kondor. 1982. Identification of a major polypeptide of the nuclear pore complex. *J. Cell Biol.* 95:826–837.

Goldberg, M. W., J. J. Blow, and T. D. Allen. 1992. The use of field emission inlens scanning electron microscopy to study the steps of assembly of the nuclear envelope in vitro. *J. Struct. Biol.* 108:257–268.

Görlich, D., F. Vogel, A. D. Mills, E. Hartmann, and R. A. Laskey. 1995. Distinct functions for the two importin subunits in nuclear import. *Nature (Lond.).* 377:246–248.

Gorsch, L. C., T. C. Dockendorff, and C. N. Cole. 1995. A conditional allele of the novel repeat-containing yeast nucleoporin RAT7/NUP159 causes both rapid cessation of mRNA export and reversible clustering of nuclear pore complexes. *J. Cell Biol.* 129:939–955.

Grandi, P., V. Doye, and E. C. Hurt. 1993. Purification of NSP1 reveals complex formation with 'GLFG' nucleoporins and a novel nuclear pore protein NIC96. *EMBO J.* 12:3061–3071.

Grandi, P., N. Schlaich, H. Tekotte, and E. C. Hurt. 1995. Functional interaction of Nic96p with a core nucleoporin complex consisting of Nsp1p, Nup49p and a novel protein Nup57p. *EMBO J.* 14:76–87.

Hallberg, E., R. W. Wozniak, and G. Blobel. 1993. An integral membrane protein of the pore membrane domain of the nuclear envelope contains a nucleoporin-like region. *J. Cell Biol.* 122:513–521.

Hinshaw, J. E., B. O. Carragher, and R. A. Milligan. 1992. Architecture and design of the nuclear pore complex. *Cell.* 69:1133–1141.

Hurt, E. C. 1988. A novel nucleoskeletal-like protein located at the nuclear periphery is required for the life cycle of *Saccharomyces cerevisiae*. *EMBO J.* 7: 4323–4334.

Hurwitz, M. E., and G. Blobel. 1995. NUP82 is an essential yeast nucleoporin required for Poly(A)+ RNA export. *J. Cell Biol.* 130:1275–1281.

Jarnik, M., and U. Aebi. 1991. Toward a more complete 3-D structure of the nuclear pore complex. *J. Struct. Biol.* 107:291–308.

Kadowaki, T., M. Hitomi, S. Chen, and A. M. Tartakoff. 1994. Nuclear mRNA accumulation causes nucleolar fragmentation in yeast mtr2 mutant. *Mol. Biol. Cell.* 5:1253–1263.

Kilmartin, J. V., and A. E. Adams. 1984. Structural rearrangements of tubulin and actin during the cell cycle of the yeast *Saccharomyces*. *J. Cell Biol.* 98: 922–933.

Knight, A. E. 1994. The diversity of myosin-like proteins. Ph.D. Thesis. Cambridge, MA.

Kraemer, D. M., C. Strambio-de-Castillia, G. Blobel, and M. P. Rout. 1995. The essential yeast nucleoporin NUP159 is located on the cytoplasmic side of the nuclear pore complex and serves in karyopherin-mediated binding of transport substrate. *J. Biol. Chem.* 270:19017–19021.

Kyte, J., and R. F. Doolittle. 1982. A simple method for displaying the hydropathic character of a protein. *J. Mol. Biol.* 157:105–132.

Lee, W.-C., Z. Xue, and T. Mélèse. 1991. The NSR1 gene encodes a protein that specifically binds nuclear localization sequences and has two RNA recognition motifs. *J. Cell Biol.* 113:1–12.

Li, O., C. V. Heath, D. C. Amberg, T. C. Dockendorff, C. S. Copeland, M. Snyder, and C. N. Cole. 1995. Mutation or deletion of the *Saccharomyces cerevisiae* RAT3/NUP133 gene causes temperature-dependent nuclear accumulation of poly(A)$^+$ RNA and constitutive clustering of nuclear pore complexes. *Mol. Biol. Cell.* 6:401–417.

Lipman, D. J., and W. R. Pearson. 1985. Rapid and sensitive protein similarity searches. *Science (Wash. DC).* 227:1435–1441.

Loeb, J. D. J., G. Schlenstedt, D. Pellman, D. Kornitzer, P. A. Silver, and G. R. Fink. 1995. The yeast nuclear import receptor is required for mitosis. *Proc. Natl. Acad. Sci. USA.* 92:7647–7651.

Lupas, A., M. Van Dyke, and J. Stock. 1991. Predicting coiled coils from protein sequences. *Science (Wash. DC).* 239:1288–1291.

Maul, G. G. 1977. The nuclear and cytoplasmic pore complex: structure, dynamics, distribution, and evolution. *Intl. Rev. Cytol. Suppl.* 6:75–186.

Moroianu, J., G. Blobel, and A. Radu. 1995*a*. Previously identified protein of uncertain function is karyopherin alpha and together with karyopherin beta docks import substrate at nuclear pore complexes. *Proc. Natl. Acad. Sci. USA.* 92:2008–2011.

Moroianu, J., M. Hijikata, G. Blobel, and A. Radu. 1995b. Mammalian karyopherin-$\alpha_1\beta$ and $\alpha_2\beta$ heterodimers: α_1 or α_2 subunit binds nuclear localization signal and β subunit interacts with peptide repeat-containing nucleoporins. *Proc. Natl. Acad. Sci. USA.* 92:6532–6536.

Nehrbass, U., H. Kern, A. Mutvei, H. Horstmann, B. Marshallsay, and E. C. Hurt. 1990. NSP1: a yeast nuclear envelope protein localized at the nuclear pores exerts its essential function by its carboxy-terminal domain. *Cell.* 61: 979–989.

Pemberton, L. F., M. P. Rout, and G. Blobel. 1995. Disruption of the nucleoporin gene NUP133 results in clustering of nuclear pore complexes. *Proc. Natl. Acad. Sci. USA.* 92:1187–1191.

Radu, A., G. Blobel, and R. W. Wozniak. 1993. Nup155 is a novel nuclear pore complex protein that contains neither repetitive sequence motifs nor reacts with WGA. *J. Cell Biol.* 121:1–9.

Radu, A., G. Blobel, and R. W. Wozniak. 1994. Nup107 is a novel nuclear pore complex protein that contains a leucine zipper. *J. Biol. Chem.* 269:17600–17605.

Radu, A., G. Blobel, and M. S. Moore. 1995. Identification of a protein complex that is required for nuclear protein import and mediates docking of import substrate to distinct nucleoporins. *Proc. Natl. Acad. Sci. USA.* 92:1769–1773.

Ris, H., and M. Malecki. 1993. High-resolution field emission scanning electron microscope imaging of internal cell structures after Epon extraction from sections: a new approach to correlative ultrastructural and immunocytochemical studies. *J. Struct. Biol.* 111:148–157.

Rose, M., P. Grisafi, and D. Botstein. 1984. Structure and function of the yeast *URA3* gene: expression in *Escherichia coli*. *Gene.* 29:113–124.

Rothstein, R. 1991. Targeting, disruption, replacement, and allele rescue: integrative DNA transformation in yeast. *Methods Enzymol.* 194:281–301.

Rout, M. P., and J. V. Kilmartin. 1990. Components of the yeast spindle and spindle pole body. *J. Cell Biol.* 111:1913–1927.

Rout, M. P., and G. Blobel. 1993. Isolation of the yeast nuclear pore complex. *J. Cell Biol.* 123:771–783.

Rout, M. P., and S. R. Wente. 1994. Pores for thought: nuclear pore proteins. *Trends Cell Biol.* 4:357–365.

Schneiter, R., T. Kadowaki, and A. M. Tartakoff. 1995. mRNA transport in

yeast: time to reinvestigate the functions of the nucleolus. *Mol. Biol. Cell.* 6: 357–370.

Sherman, F., G. R. Fink, and J. B. Hicks. 1986. Methods in Yeast Genetics. Cold Spring Harbor Laboratory, Cold Spring Harbor.

Stutz, F., M. Neville, and M. Rosbash. 1995. Identification of a novel nuclear pore-associated protein as a functional target of the HIV-1 Rev protein in yeast. *Cell.* 82:495–506.

Uhlen, M., B. Guss, B. Nilsson, S. Gatenbeck, L. Philipson, and L. M. 1984. Complete sequence of the staphylococcal gene encoding protein A. A gene evolved through multiple duplications. *J. Biol. Chem.* 259:1695–1702.

Unwin, P. N., and R. A. Milligan. 1982. A large particle associated with the perimeter of the nuclear pore complex. *J. Cell Biol.* 93:63–75.

Wente, S. R., and G. Blobel. 1993. A temperature-sensitive NUP116 null mutant forms a nuclear envelope seal over the yeast nuclear pore complex thereby blocking nucleocytoplasmic traffic. *J. Cell Biol.* 123:275–284.

Wente, S. R., and G. Blobel. 1994. NUP145 encodes a novel yeast glycine-leucine-phenylalanine-glycine (GLFG) nucleoporin required for nuclear envelope structure. *J. Cell Biol.* 125:955–969.

Wente, S. R., M. P. Rout, and G. Blobel. 1992. A new family of yeast nuclear pore complex proteins. *J. Cell Biol.* 119:705–723.

Winey, M., C. L. Mamay, E. T. O'Toole, D. N. Mastronarde, T. H. J. Giddings, K. L. McDonald, and J. R. McIntosh. 1995. Three-dimensional ultrastructural analysis of the Saccharomyces cerevisiae mitotic spindle. *J. Cell Biol.* 129:1601–1615.

Wozniak, R. W., E. Bartnik, and G. Blobel. 1989. Primary structure analysis of an integral membrane glycoprotein of the nuclear pore. *J. Cell Biol.* 108: 2083–2092.

Wozniak, R. W., G. Blobel, and M. P. Rout. 1994. POM152 is an integral protein of the pore membrane domain of the yeast nuclear envelope. *J. Cell Biol.* 125:31–42.

Wu, J., M. J. Matunis, D. Kraemer, G. Blobel, and E. Coutavas. 1995. Nup358, a cytoplasmically exposed nucleoporin with peptide repeats, Ran-GTP binding sites, zinc fingers, a cyclophilin A homologous domain, and a leucine-rich region. *J. Biol. Chem.* 270:14209–14213.

Yang, C. H., E. J. Lambie, J. Hardin, J. Craft, and M. Snyder. 1989. Higher order structure is present in the yeast nucleus: autoantibody probes demonstrate that the nucleolus lies opposite the spindle pole body. *Chromosoma.* 98:123–128.

Yano, R., M. Oakes, M. Yamaghishi, J. A. Dodd, and M. Nomura. 1992. Cloning and characterizatrion of SRP1, a suppressor of temperature-sensitive RNA polymerase I mutations, in *Saccharomyces cerevisiae. Mol. Cell. Biol.* 12:5640–5651.